

## Article

# The Study of Hydrogen Volume Fraction Effects on the Flame Temperature of Turbulence Diffusion Propane Jet Flames

Bingchuan Yan <sup>1</sup>, Chao Sun <sup>1</sup>, Qingshan Feng <sup>2</sup>, Jian Chen <sup>1</sup>, Yuke Gao <sup>3</sup> and Changfa Tao <sup>3,\*</sup>

<sup>1</sup> Pipe China North Pipeline Co., Ltd., Langfang 065000, China; yanbc@pipechina.com.cn (B.Y.); sunchaosky@163.com (C.S.); chenjian@pipechina.com.cn (J.C.)

<sup>2</sup> China Oil & Gas Pipeline Network Corporation, Beijing 100013, China; fengqs@pipechina.com.cn

<sup>3</sup> School of Automotive and Transportation Engineering, Hefei University of Technology, Hefei 230009, China; ykgao@mail.dlut.edu.cn

\* Correspondence: chftao84@hfut.edu.cn

**Abstract:** This paper studies the influence of hydrogen volume fraction effects on the temperature distribution of diffusion turbulent propane jet flames. Numbers of experimental scenarios have been carried out to investigate the evolution of temperature distribution under different hydrogen volume fractions. In the continuous region, these experimental results show that the temperature distribution and the maximum temperature of diffusion of turbulent jet flames are proportional to the hydrogen volume fraction under the same heat release rate of propane. Considering the model of virtual point source and the three-stage model, the theoretical model between the hydrogen volume fraction and flame temperature has been analyzed. The relationship among the temperature distribution, hydrogen volume fraction, and heat release rate has been modified. It can provide some important references for the fire risk assessment of turbulent diffusion jet flames.

**Keywords:** hydrogen; temperature distribution; turbulence diffusion jet flames; virtual point source



**Citation:** Yan, B.; Sun, C.; Feng, Q.; Chen, J.; Gao, Y.; Tao, C. The Study of Hydrogen Volume Fraction Effects on the Flame Temperature of Turbulence Diffusion Propane Jet Flames. *Fire* **2024**, *7*, 10. <https://doi.org/10.3390/fire7010010>

Academic Editor: Ali Cemal Benim

Received: 24 October 2023

Revised: 1 December 2023

Accepted: 20 December 2023

Published: 25 December 2023



**Copyright:** © 2023 by the authors. Licensee MDPI, Basel, Switzerland. This article is an open access article distributed under the terms and conditions of the Creative Commons Attribution (CC BY) license (<https://creativecommons.org/licenses/by/4.0/>).

## 1. Introduction

In recent years, hydrogen (H<sub>2</sub>) has been widely used to add into hydrocarbon fuel gas to improve its combustion processes [1,2]. The jet flames of H<sub>2</sub> and of hydrocarbon fuel present very different characteristics, such as their burning velocities, heat release rates, flame blow-off velocities, air entrainment rate, flame lift-off height, thermal radiation fraction, flame temperature, and propensities to flame quenching. However, the gas mixture, which contains H<sub>2</sub>, has some significant safety issues since the explosive limit of H<sub>2</sub> is 4–75.6%. Furthermore, these high-pressure pipelines will be eroded much more easily since the hydrogen causes embrittlement. The turbulent diffusion jet flames of gas mixtures will be observed once the high-pressure pipelines leak. As discussed in previous studies, the flame temperature is the crucial parameter that will seriously influence the fire development. The addition of H<sub>2</sub> will inevitably influence their temperature fields [3]. Therefore, it is of great significance to accurately predict the flame temperature of gas mixtures that contain H<sub>2</sub>.

In previous studies, the main focus has been on the flame temperature of turbulence diffusion jet fire for pure fuels [4–7]. Hyun et al. [4] measured the soot volume fraction and the soot temperature profiles and used spectral soot emission to study the sensitivity of soot formation to pressure in co-flow laminar diffusion flames. They found that radial temperature gradients within the flame increased with pressure above the burner rim. It was also found that higher radial temperature gradients near the burner exit at higher pressures. Hu et al. [5] conducted experiments in Lhasa and Hefei to investigate the influence of atmospheric pressure on the axial temperature of diffusion turbulent jet flames. They found that the maximum value of flame temperature under the ambient pressure was higher than the ones of low ambient pressure. The classical three-section buoyancy-induced

flow model modified by the virtual point source was used to develop the dimensionless temperature model under different ambient pressures. Zhang et al. [6] analyzed the temperature distribution in the vertical direction of the jet flame buoyancy control region while the rectangular burners with different aspect ratios and heat release rates were considered. They assumed that the centerline temperature of buoyancy control was a function of the Froude number, which was related to the outlet velocity. Mercedes et al. [7] studied the centerline temperature of larger-scale diffusion jet flames in the vertical direction, and they found the functional relationship between the centerline temperature value and their locations. McCaffrey [8] analyzed the jet flames, and he obtained the classic three-section distribution model of the fire. The temperature in the vertical direction of jet flames can also be divided into three regions: continuous flame region, intermittent flame region, and plume region. The axial temperature distribution of jet flames could be effectively described by the dimensionless three-section theory [9,10]. Liu et al. [10] investigated the plume centerline temperature of pool fire under different ullage heights (distance between the fuel surface and the burner upper rim). They found that the plume centerline temperature decreases with the ullage height under minor ullage height conditions. It increases with a further increase in the ullage height due to the increase in the air entrainment rate, which advances the local burning intensities of the fire plume. Wang et al. [11] conducted plenty of experiments on turbulent diffusion jet flames under different tilt angles, and they analyzed the temperature distribution on the flame centerline. These experimental results showed that the flame temperature decreased with an increase in the inclined angle. A parameter of the tilt angle has been considered to add into the classical model for establishing a new dimensionless correlation. The virtual point source of jet flames has been defined as: there is a point below or above the fire source, which can be regarded as the point of heat release. Therefore, the virtual point source is always used for correcting the temperature distribution of jet flames [9]. Xing et al. [12] analyzed the heat transfer of buoyancy turbulent diffusion flames under two different air entrainment conditions. The experimental results indicated that the air entrainment rate of the jet flames near the wall was much lower than that of the free flames. Wang et al. [13] studied the evolution of axisymmetric diffusion jet flames constrained by parallel side walls. Tao et al. [14] analyzed the characteristics of the virtual point source of jet flames under different side wall spaces, and they have established a correlation model between the virtual point source and side wall distance using the hydraulic diameter. They found that the virtual origin of buoyancy-controlled jet flames was always larger than 0, which increased in reducing the spaces of sidewalls. And the virtual origin increased with the heat release rate. A global model has been proposed to estimate the virtual origin of jet flames. Gong et al. [15] conducted a series of ignited release experiments for cryogenic hydrogen at different release pressures and release temperatures. They found that the jet flame temperature of cryogenic hydrogen increases with an increase in the release pressure and a decrease in the release temperature. Furthermore, the critical separation distance can be calculated based on the jet flame temperature on the centerline. A dimensionless relationship for the temperature distribution of the cryogenic hydrogen jet flame has been developed that presents a three-region distribution, which is similar to the ambient temperature of jet flames.

Some works about the combustion characteristics of gas mixtures have been carried out [16–20]. Zhao et al. [16] investigated the flame height, flame width, and lift-off height of blended  $H_2/CH_4$  non-premixed jet flames. They found that the flame height decreases with an increase in the  $H_2$  volume fraction ( $f_{v,H_2}$ ) while their flame width versus flame height was not self-similar. They also developed a new correlation of lift-off height under different  $f_{v,H_2}$ . Kong et al. [17] studied the jet flame characteristics of  $H_2/CH_4$  in the horizontal direction. The temperature distribution in the horizontal axis can be characterized by the classical centerline temperature relation of the free fire. The lift-off length decreased with the addition of  $H_2$ , while the flame length under different conditions has been analyzed and quantified. Li et al. [18] proposed a solid flame model of thermal radiation to calculate the safe separation distance of  $H_2/CH_4$  mixtures pipeline jet flame. They developed a

new model to solve the calculation problem of the near-field view factor, which agreed well with the experimental results. He et al. [19] investigated the centerline temperature of hydrogenated fuel gas under free and wall fire conditions. The vertical temperature of jet flames was proportional to the  $f_{v,H_2}$ , while the flame height was inversely proportional to it. They also found that the virtual origin increased with the volume ratio of  $H_2$ , and the virtual point source of jet flames near the wall was significantly larger than the ones of the free flame. Tang et al. [20] studied the combustion characteristics of  $H_2$  jet flames under varying  $N_2$  dilution concentrations and nozzle diameters. The flame height of  $H_2$  jet flames under the same heat release rate decreased with increased dilution concentration due to enhanced air entrainment. The lift-off distance was independent of the nozzle diameter for the jet flame at the same dilution concentration but increased with the dilution concentration due to the decrease in the flame combustion speed.

The characteristics of flame temperature of the pure fuel gas under different boundary conditions have been studied for decades. Moreover, the combustion characteristics of  $H_2/CH_4$  gas mixtures have been investigated, such as flame height, flame width, and lift-off height. The flame temperature in the horizontal direction has also been investigated but without the ones in the vertical direction. The flame temperature distribution under different directions will be very different, especially for the  $H_2$  and hydrocarbon gas mixtures. In this study, a series of experiments about the centerline temperature of turbulence diffusion jet flames of the  $H_2$  and propane ( $C_3H_8$ ) gas mixtures have been carried out. The virtual point source has been considered with the same flow rate of  $C_3H_8$  under different  $f_{v,H_2}$ . It can be found that the value of the virtual point source decreases with an increase in  $f_{v,H_2}$ . The virtual point source method for the fire plume has also been analyzed, firstly for the gas mixture. Based on the classic three-region theory, a modified correlation, which considered the effect of  $f_{v,H_2}$ , has been developed. This correlation can accurately predict the flame temperature of gas mixtures.

## 2. Experimental Setup

In order to investigate the combustion characteristics of  $C_3H_8-H_2$  diffusion jet flames with different  $f_{v,H_2}$ , an experimental setup was built, as shown in Figure 1. The experimental setup includes a gas supply system, a flow control system, nozzles, and a temperature acquisition system. Before igniting the fuel gas, the temperature acquisition device was turned on. The flow rates of  $C_3H_8$  and  $H_2$  were controlled by flow meters, respectively. The gas mixing tank was used for mixing the gases completely. Two nozzles, whose diameters ( $D$ ) are 2 and 3 mm, were used. To ensure the repeatability of experimental results, each experimental scenario was repeated 3 times under the quietest conditions. The ambient temperature was at  $15 \pm 2$  °C, while the ambient pressure was  $101 \pm 5$  kPa. As shown in Figure 1, about 16 K-thermocouples with the accuracy of  $\pm 1$  °C were fixed as a thermocouple tree upon the nozzle. This is the usual method for the study of fire dynamics, which is considered in many papers [5,6,13,14]. The distances between each thermocouple and the nozzle are 0.05, 0.10, 0.15, 0.20, 0.25, 0.35, 0.45, 0.55, 0.65, 0.75, 0.85, 0.95, 1.05, 1.15, 1.25, and 1.35 m. It is noted that there is a radiation error in temperature measurement using thermocouples [21]. Therefore, the true value of the flame temperature can be calculated using thermocouple measurements, considering the heat transfer model [22,23]. The data acquisition device was connected with 16 K-type thermocouples, while it was also connected with PC for collecting and processing data in real time. Every experimental scenario lasted for 120 s. All of the experimental scenarios are shown in Table 1.

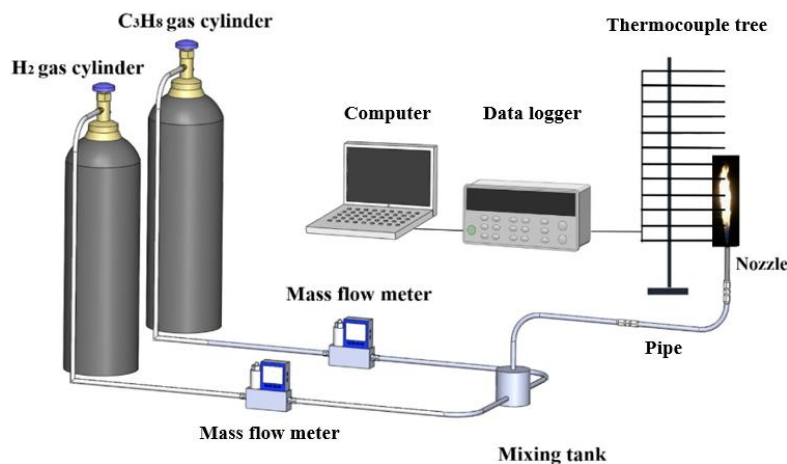


Figure 1. The schematic of the experimental setup.

Table 1. The summary of the experimental scenarios.

$D$ (mm)	$C_3H_8$ (m <sup>3</sup> /h)	$H_2$ (m <sup>3</sup> /h)	$\dot{Q}_{C_3H_8}$ (kW)
2	0.077, 0.116, 0.155, 0.232	0, 0.114, 0.227, 0.341, 0.455, 0.568	2.176, 3.264, 4.352, 6.755
3	0.077, 0.124, 0.155, 0.232, 0.279, 0.310, 0.341, 0.372	0, 0.068, 0.091, 0.114, 0.136, 0.159, 0.182, 0.205, 0.227, 0.341, 0.455, 0.568	2.176, 3.482, 4.532, 6.529, 7.835, 8.705, 9.576, 10.447

The flame temperature is measured by the K-type thermocouples with some heat loss caused by the thermal radiation, which could not give the absolute temperature. Then, the flame temperature should be revised according to the thermal radiation. It can be revised by Equation (1), while the radiation correction has been considered [24]:

$$T_g - T_{th} = \frac{\sigma \epsilon (1 - \epsilon_g) T_g^4}{h + 4\sigma \epsilon T_g^3} \tag{1}$$

where  $T_g$  is the gas temperature,  $T_{th}$  is the absolute temperature reading of the thermocouple,  $h$  is the convective heat transfer coefficient for the thermocouple junction,  $\sigma$  is the Stefan–Boltzmann constant,  $\epsilon$  and  $\epsilon_g$  are, respectively, the emissivity of the thermocouple and the gas, and they are assumed to be 0.9 and 0.1 [25,26]. The thermocouple junction is assumed to be a cylinder, and  $h$  is given by  $Nu = 0.43 + 0.53Re^{0.5}Pr^{0.31}$  [27]. The measured velocities are used to calculate the Reynolds (Re) number. The flame temperature was recorded for about 120 s with stable combustion, which shows small deviations with respect to their mean temperature (about 3.1%), with the fine control of the gas flow rate of the jet flame.

### 3. The Experimental Results and Discussion

Figure 2 shows the flame temperature curves of the centerline under different heights. It could be found that the value of the flame temperature in the continuous region is the highest. The flame temperature was significantly influenced by the  $H_2$  at the continuous flame region. Figure 2 shows that the flame temperature of the jet flame at the continuous region increases overall with the increase in  $f_{v,H_2}$ . The increase rate of the flame temperature at the intermittent flame region and plume region is much smaller than the ones of the continuous region. This is because the outlet velocity ( $u$ ) from the nozzles increases with an increase in  $f_{v,H_2}$ , which brings a larger value of the air entrainment rate [28]. The flame height is inversely proportional to the air entrainment rate [29]. The heat release rate of  $C_3H_8$  ( $\dot{Q}_{C_3H_8}$ ) can be recognized as a constant, while the heat release rate of  $H_2$

( $\dot{Q}_{H_2}$ ) increases. Therefore, the total heat release rate ( $\dot{Q}_t$ ) of  $C_3H_8$ — $H_2$  diffusion jet flames increases. It can be deduced that the chemical energy of the fuel gas released mainly in the continuous region. For the diffusion jet flames of gas mixtures, there are three effects, which are dilution, heat, and chemical effects [30].

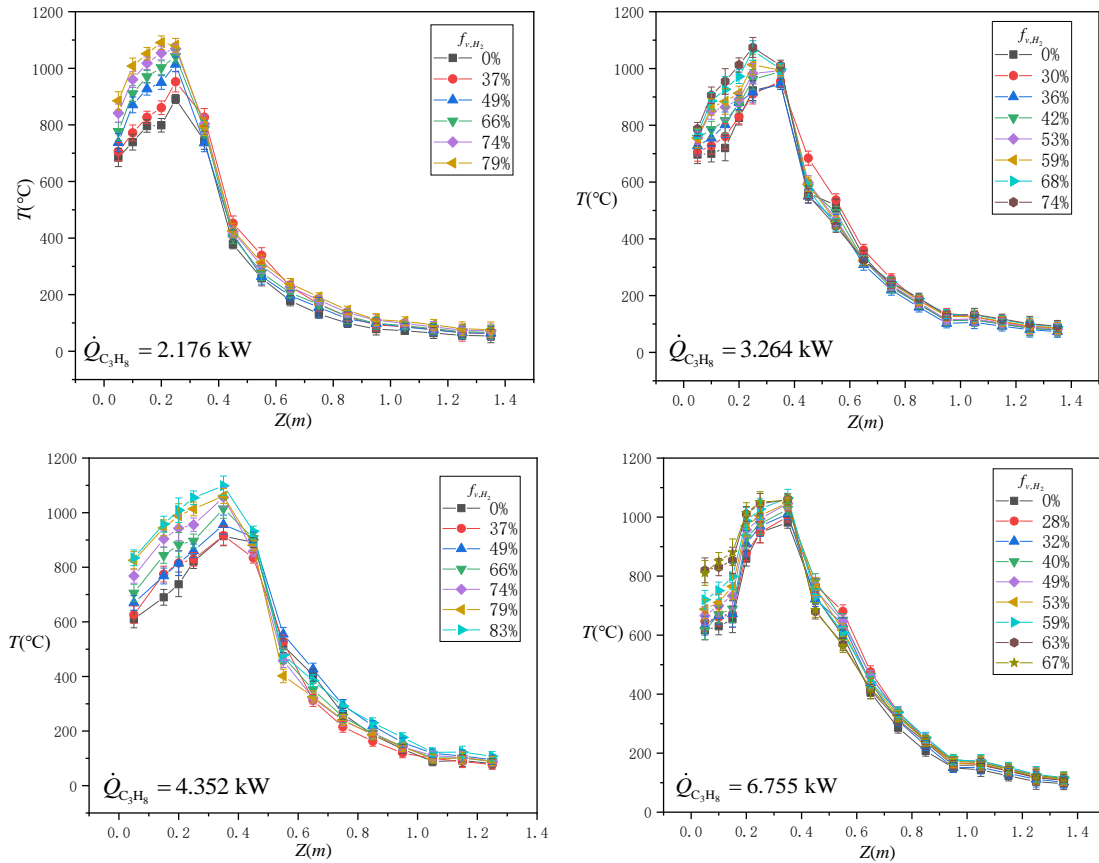


**Figure 2.** The evolution of centerline temperature of jet flames for  $D = 2$  mm.

With the addition of  $H_2$ , the heat effect is much more obvious than the dilution effect. In addition, the ignition energy of  $H_2$  is the lowest for all of the combustion materials. Then, the  $C_3H_8$  will burn much more completely due to its chemical effects of gas mixtures. As discussed in Ref [31], the effects of the  $H_2$  mole fraction on the chemical reaction have been discussed. The main reaction pathways are  $C_3H_8 \rightarrow N-C_3H_7 \rightarrow C_2H_4 \rightarrow CH_3 \rightarrow CH_2O \rightarrow HCO \rightarrow CO \rightarrow CO_2$  and  $C_3H_8 \rightarrow I-C_3H_7 \rightarrow C_3H_6 \rightarrow CH_3 \rightarrow CH_2O \rightarrow HCO \rightarrow CO \rightarrow CO_2$ . It shows that the H-atom abstractions of propane are affected by the additional hydrogen. With a decrease in propane, the percentage of  $N-C_3H_7$  formation will increase, while the  $I-C_3H_7$  percentage is reduced through the reaction of  $C_3H_8 + H = I-C_3H_7 + H_2$ ,  $C_3H_8 + O = I-C_3H_7 + OH$ , and  $C_3H_8 + OH = I-C_3H_7 + H_2O$ . The HCO production way is affected by the  $H_2$  addition, while its production value of reaction  $CH_2O + H = HCO + H_2$  is reduced, and the  $CH_2O + OH = HCO + H_2O$  improves it with a decrease in the  $H_2$  volume fraction. The reaction paths containing OH and H radicals are affected by the  $H_2$  fraction reduction. Hence, the effects of the  $H_2$  mole fraction affect the reaction pathways by the OH and H radical production, resulting in varied flame structures and different thermal performances. The OH radicals are produced by  $H + O_2 = OH + O$ ,  $H_2O + O = 2OH$ , and  $H_2 + O = OH + H$ . The addition of  $H_2$  contributes to the H radical production through  $H_2 = OH + H$  and  $H_2 + O = OH + H$ , while it restrains the H formation from  $CH_3 + O = CH_2O + H$ ,  $HCO + M = CO + H + M$ , and  $CO + OH = CO_2 + H$ . Based on that analysis, Peng et al. [31] studied the reaction pathways effected by the  $H_2$  mole fraction.

It is noted that the flame temperature increases significantly with the H<sub>2</sub> dilution concentration. This experimental result is reasonable since an increase in dilution concentration increases the heat release rate of H<sub>2</sub>. The flame brightness decreases, which changes to blue, with H<sub>2</sub> dilution concentration. The intensity of the blue flame is determined by the square of the hydroxyl (OH) concentration [32].

According to the equations of mass, momentum, and energy, the temperature difference distribution between the flame and ambient in the vertical direction of jet flames can be expressed as [10,33]:

$$\Delta T_Z = K\alpha^{-4/3} \left( \frac{\dot{Q}}{c_p \rho_0} \right)^{2/3} Z^{-5/3} T_0^{1/3} \tag{2}$$

According to the dimensionless analysis, Equation (2) can be written as:

$$\frac{T_z - T_0}{T_0} = K\alpha^{-4/3} Q^{*2/3} D^{-5/3} Z^{-5/3} \tag{3}$$

where  $\alpha$  is the entrainment coefficient rate, and  $\dot{Q}^*$  is the dimensional heat release rate. From Equations (2) and (3), it can be seen that the temperature of jet flames is influenced by the air entrainment rate.

Figure 3 shows the temperature differences of the flame centerline under different  $D$  when  $\dot{Q}_{C_3H_8} = 2.176$  kW. It can be found that the evolution of centerline temperature jet flames with different diameters is very different. The  $u$  from the nozzle will be the largest when  $D$  is the smallest one under the same  $\dot{Q}_t$ . There will be much more vortexes near the nozzle while the flow stage becomes the full turbulence flow. For the turbulent flow, more vortexes will be found near the nozzle. In addition, the vortical activity increases with the  $u$ . Then, more air will be entrained into the flame body. Thus, the air entrainment rate will increase proportionally to the  $u$ . The C<sub>3</sub>H<sub>8</sub> in the gas mixture will be consumed fast, which is another reason for the increase in the centerline temperature in the continual region. The maximum temperature is proportional to the  $f_{v,H_2}$  under the same  $\dot{Q}_{C_3H_8}$ .

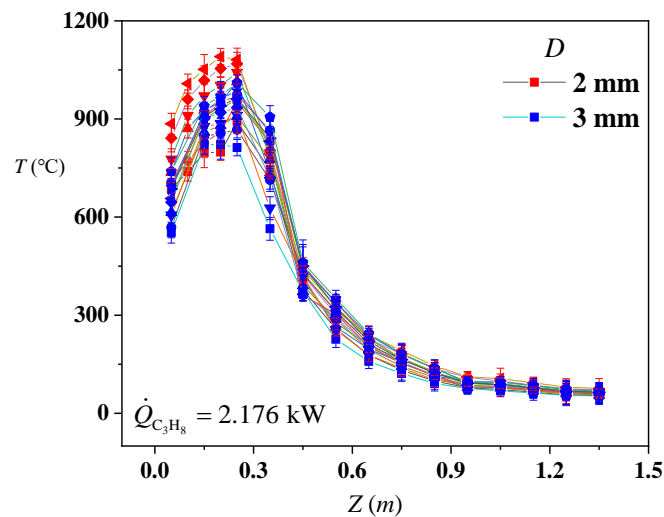


Figure 3. Comparison of centerline temperature under the same  $\dot{Q}_{C_3H_8}$  and different  $D$ .

Figure 4 shows the variation of the maximum temperature ( $T_{max}$ ) of the centerline temperature under different volume flow rates of C<sub>3</sub>H<sub>8</sub> and H<sub>2</sub>. It can be clearly observed that  $T_{max}$  is proportional to  $\dot{Q}_t$  of mixed fuel when the volume flow rate of C<sub>3</sub>H<sub>8</sub> is constant. The maximum value of the temperature difference ( $\Delta T_{max}$ ) reaches about 200 °C with an increase in  $f_{v,H_2}$ . It can be found that the  $\Delta T_{max}$  increases slightly when  $f_{v,H_2} < 0.6$ , but

it increases sharply when  $f_{v,H_2} \geq 0.6$ ; it is also a turning point for the thermal radiation fraction [34]. According to the previous studies [35,36], the addition of H<sub>2</sub> brings some common experimental phenomenon. The combustion characteristics will be dominated by hydrocarbon fuel when  $f_{v,H_2} < 0.6$ , while they will be dominated by H<sub>2</sub> when  $f_{v,H_2} \geq 0.6$ .

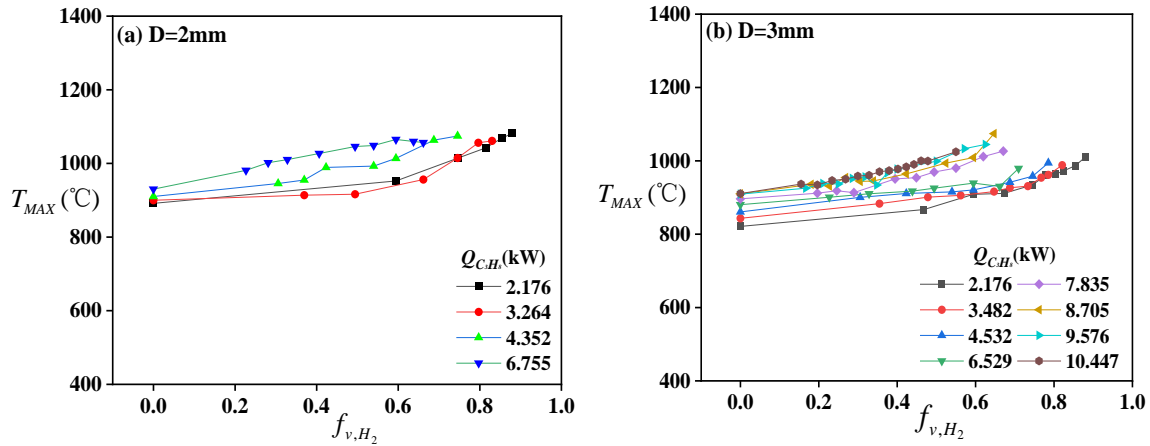


Figure 4. Effect of hydrogen gas on maximum flame temperature.

In the previous study, the temperature distribution in the plume region is analyzed by the virtual point source method [10,37]. The virtual point source can be explained as: there is a virtual point below or upon the real fire source which releases the combustion heat [37]. According to the virtual point model, the height can be revised to a more accurate value for the flame temperature. By replacing the height  $Z$  in the plume temperature formula with the corrected height [10,33], it can be obtained that:

$$\Theta = \frac{(T_z - T_0)/T_0}{\left(\frac{\dot{Q}}{\rho_0 c_p T_0 g^{1/2} D^{5/2}}\right)^{2/3}} = \frac{\Delta T_z/T_0}{\dot{Q}^{*2/3}} = fcn\left(\frac{Z - Z_0}{D}\right) \tag{4}$$

where  $T_z$  is the flame temperature at different heights,  $\rho_0$  is the ambient density,  $T_0$  is the ambient temperature, and  $Z_0$  is the value of the virtual point source.  $Z$  is the heights at random locations. For axisymmetric plumes:

$$\Theta = \frac{\Delta T_z/T_0}{\dot{Q}^{*2/3}} \propto \left(\frac{Z - Z_0}{D}\right)^{-5/3} \tag{5}$$

This equation can be rewritten as:

$$\Phi = \left(\frac{\dot{Q}^{*2/3}}{\Delta T_z/T_0}\right)^{3/5} \propto (Z - Z_0) \tag{6}$$

Thus, there is a linear relationship between  $\Phi = \left(\dot{Q}^{*2/3}/(\Delta T_z/T_0)\right)^{3/5}$  and  $Z - Z_0$ , and the intercept of the straight line formed by the data points on the axis in Figure 5 represents the virtual point source.

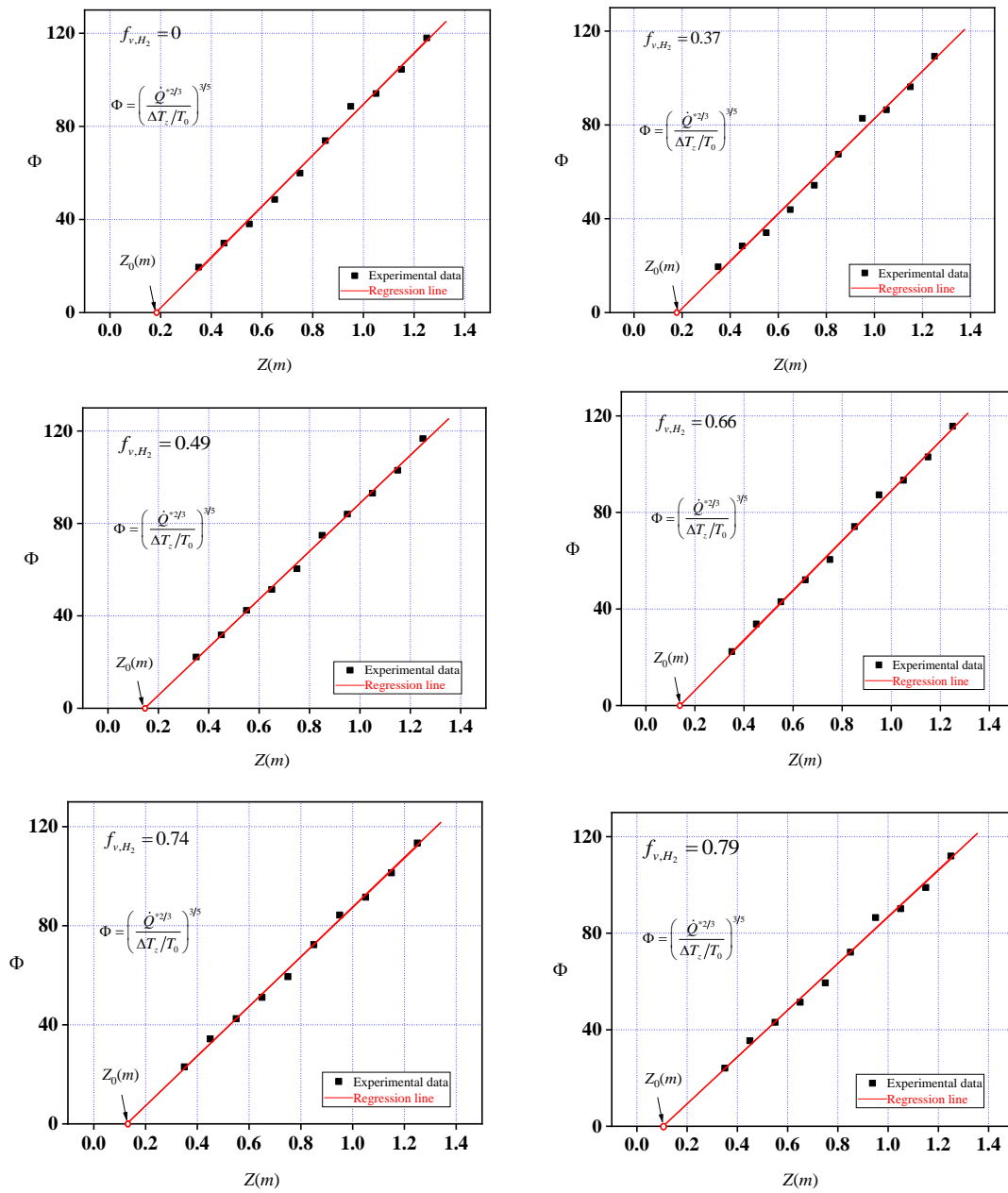


Figure 5. Derivation of a virtual point source when  $\dot{Q}_{C_3H_8} = 3.264$  kW and  $D = 2$  mm.

Figure 5 shows the typical experimental results of the virtual point source for the 2 mm diameter nozzle while  $\dot{Q}_{C_3H_8} = 3.264$  kW. It can be seen that all the  $Z_0$  are greater than 0, which means that  $Z_0 > 0$ . The increase in  $f_{v,H_2}$  will reduce the value of  $Z_0$ . The  $\dot{Q}_{C_3H_8}$  is a constant, while the  $\dot{Q}_{H_2}$  increases with an increase in  $f_{v,H_2}$  and  $\dot{Q}_t$  increases. As discussed in the previous text, the air entrainment rate is proportional to the turbulence intensity, which will increase the flame temperature and reduce the flame height. As a result, the value of  $\Phi$  decreases since the  $\Delta T_z$  increases sharply.

Moreover, its position moves closer to the nozzle. This suggests that the addition of  $H_2$  has a certain impact on the virtual point source, which is essentially due to the concentration of flame energy release below the flame.

A virtual point source is a function of the  $\dot{Q}_t$ , temperature difference ( $\Delta T_f$ ), and  $D$  [28], which can be expressed as:

$$Z_0 = fcn(\dot{Q}, \Delta T_f, D) \quad (7)$$

After introducing the virtual point source, the flame temperature in the vertical direction can be fitted through the following the relationship:

$$\frac{(T_z - T_0)}{T_0} \sim \frac{(Z - Z_0)/D}{\dot{Q}^{*2/5}} \tag{8}$$

As discussed in the previous text, the value of  $Z_0$  decreases with an increase in  $f_{v,H_2}$  while the flame temperature increases. Then,  $(T_z - T_0)/T_0$  is proportional to  $f_{v,H_2}$ . But in fact, the value of  $(Z - Z_0)/D \dot{Q}^{*2/5}$  changes slightly under the same  $\dot{Q}_{C_3H_8}$  and  $f_{v,H_2}$ . Based on that,  $f_{v,H_2}$  is an important parameter to influence the dimensionless model. Here, the addition of a new parameter  $(1/(1 + f_{v,H_2}))^{2/5}$  has been considered, which has been carried out [37]. Then, it gives:

$$\left(\frac{1}{1 + f_{v,H_2}}\right)^{2/5} \frac{(T_z - T_0)}{T_0} \sim \frac{(Z - Z_0)/D}{\dot{Q}^{*2/5}} \tag{9}$$

The variation of the central axis temperature of turbulence diffusion jet flames of  $C_3H_8$  and  $H_2$  gas mixtures has been analyzed according to the three-stage theory proposed by McCaffrey [8]. These three stages are continuous region, intermittent flame region, and plume region. The flame temperature of the continuous region changes slightly with an increase in height, while it decreases with a different rate for the intermittent region and plume region. As shown in Figure 6, each experimental data converges to the fitting curve highly. For the pure fuel, the applicability of the classical three-stage model proposed by McCaffrey [8] can describe the evolution of the flame temperature well. And the experimental data in this study overlap the ones obtained by McCaffrey in Figure 6.

$$\begin{cases} \left(\frac{1}{1 + f_{v,H_2}}\right)^{2/5} \frac{(T - T_0)}{T_0} = 0.115 \left[\frac{(Z - Z_0)/D}{\dot{Q}^{*2/5}}\right] + 2.442 & \frac{(Z - Z_0)/D}{\dot{Q}^{*2/5}} \leq 2.3 \end{cases} \tag{10a}$$

$$\begin{cases} \left(\frac{1}{1 + f_{v,H_2}}\right)^{2/5} \frac{(T - T_0)}{T_0} = 13.8 \left[\frac{(Z - Z_0)/D}{\dot{Q}^{*2/5}}\right]^{-1.6} & \frac{(Z - Z_0)/D}{\dot{Q}^{*2/5}} \geq 2.3 \end{cases} \tag{10b}$$

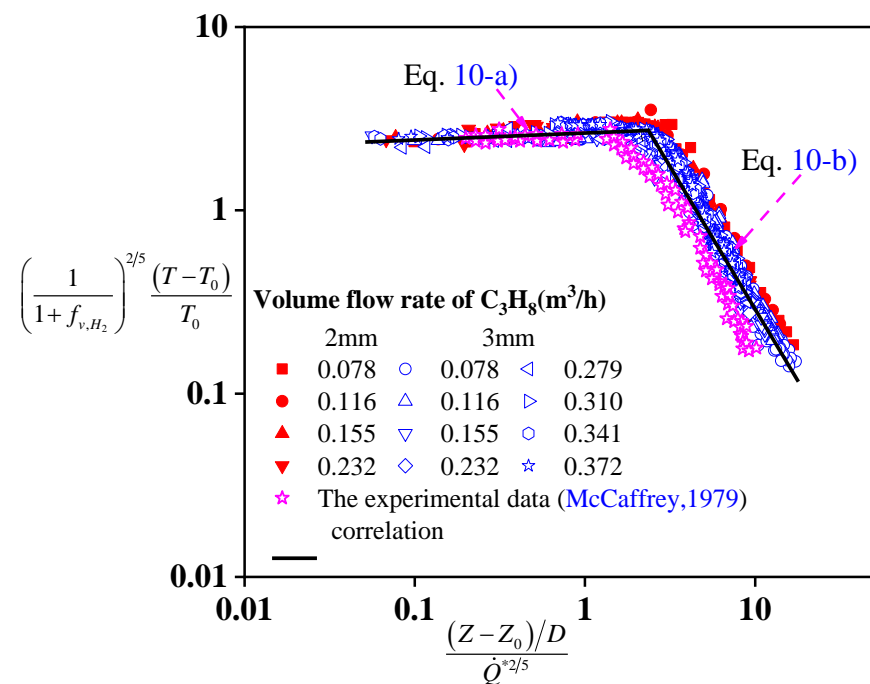


Figure 6. The modified result of dimensionless flame population distribution [8].

Based on Equation (9) and the experimental data, the flame temperature of the gas mixture of  $C_3H_8$  and  $H_2$  can be divided into two regions. In the continuous flame region, the flame temperature increases by about 200 °C. Considering the influence of  $H_2$ , a new dimensionless temperature difference has been developed, which remains as a constant, and is written as Equation (10). But for the intermittent flame region and buoyant plume region, the power value of this relationship between the dimensionless temperature difference and dimensionless height is  $-1.6$ . This dimensionless model can be used for calculating the flame temperature according to the analysis of the heat release rate, the virtual point source, the nozzle diameter, and the volume rate of  $H_2$ . It will be helpful for the fire risk assessment of the high-pressure gas pipeline and storage tank.

#### 4. Conclusions

The flame temperature in the centerline of turbulent jet flames of hydrogen-propane gas mixtures at ambient temperature and pressure (300 K, 1 bar) was studied. For the pure fuel, the experimental data agrees well with the ones obtained in the previous studies. The main conclusions can be obtained as follows:

1. The addition of hydrogen increases the centerline temperature of the turbulence diffusion jet flame. The maximum temperature increases obviously in the continuous flame region and increases slightly in the intermittent flame region and plume region.
2. It was found that the virtual point source moves downward gradually with the increase in the hydrogen volume fraction, since the flame height decreases and the flame temperature in the plume region decreases.
3. Based on the three-stage theory model, a new dimensionless model of flame temperature for the hydrogen-propane gas mixture has been proposed to describe the influence of hydrogen. The flame temperature of turbulent diffusion jet flames for the gas mixture of hydrogen-propane can be predicted accurately.

In this study, only the vertical jet flame has been considered with two circular nozzles, while both the direction and geometrical shape of the leakage fire is variable. In the future, the leakage fire with a different direction and geometrical shape will be carried out. In order to understand the combustion characteristics comprehensively, the flame temperature, flame length, flame radiation, and the other parameters will be investigated for different directions and geometrical shapes.

**Author Contributions:** Validation, formal analysis, investigation, data curation, writing—original draft preparation, visualization, B.Y.; investigation, data curation, writing—original draft preparation C.S.; conceptualization, methodology, writing—review and editing, Q.F.; conceptualization, methodology, writing—review and editing, visualization, J.C.; investigation, data curation, writing—review and editing, visualization, Y.G.; conceptualization, methodology, writing—review and editing, funding acquisition, C.T. All authors have read and agreed to the published version of the manuscript.

**Funding:** The work was financially supported by the Scientific and Technology Foundation of the National Pipe Network (No. WZXGL202105).

**Institutional Review Board Statement:** Not applicable.

**Informed Consent Statement:** Not applicable.

**Data Availability Statement:** Data are contained within the article.

**Conflicts of Interest:** The authors declare that this study received funding from Co., Ltd. The funder was not involved in the study design, collection, analysis, and interpretation of data, the writing of this article, or the discussion to submit it for publication.

## References

1. Palacios, A.; Bradley, D. Conversion of natural gas jet flame burners to hydrogen. *Int. J. Hydrogen Energy* **2021**, *46*, 17051–17059. [[CrossRef](#)]
2. Kumar, P.; Mishra, D.P. Effects of bluff-body shape on LPG–H<sub>2</sub> jet diffusion flame. *Int. J. Hydrogen Energy* **2008**, *33*, 2578–2585. [[CrossRef](#)]
3. Gu, M.Y.; Chu, H.Q.; Liu, F.S. Effects of simultaneous hydrogen enrichment and carbon dioxide dilution of fuel on soot formation in an axisymmetric coflow laminar ethylene/air diffusion flame. *Combust. Flame* **2016**, *166*, 216–228. [[CrossRef](#)]
4. Joo, H.I.; Gülder, Ö.L. Soot formation and temperature field structure in co-flow laminar methane–air diffusion flames at pressures from 10 to 60 atm. *Proc. Combust. Inst.* **2009**, *32*, 769–775. [[CrossRef](#)]
5. Hu, L.H.; Wang, Q.; Tang, F.; Delichatsios, M.; Zhang, X.C. Axial temperature profile in vertical buoyant turbulent jet flame in a reduced pressure atmosphere. *Fuel* **2013**, *106*, 779–786. [[CrossRef](#)]
6. Zhang, X.C.; Hu, L.H.; Zhu, W.; Zhang, X.L.; Yang, L.Z. Axial temperature profile in buoyant plume of rectangular source fuel jet flame in normal- and a sub-atmospheric pressure. *Fuel* **2014**, *134*, 455–459. [[CrossRef](#)]
7. Gómez-Mares, M.; Muñoz, M.; Casal, J. Axial temperature distribution in vertical jet flames. *J. Hazard. Mater.* **2009**, *172*, 54–60. [[CrossRef](#)] [[PubMed](#)]
8. McCaffrey, B.J. Purely Buoyant Diffusion Flames: Some Experimental Results. In *Final Report, Chemical and Physical Processes in Combustion*; The National Institute of Standards and Technology (NIST): Miami Beach, FL, USA, 1979; p. 49.
9. Karlsson, B.; Quintiere, J.G. *Enclosure Fire Dynamics*; CRC Press LLC: Boca Raton, FL, USA, 2000.
10. Liu, C.X.; Ding, L.; Ji, J. Experimental study of the effects of ullage height on fire plume centerline temperature with a new virtual origin model. *Process Saf. Environ. Prot.* **2021**, *146*, 961–967. [[CrossRef](#)]
11. Wang, Q.; Yan, J.; Wang, B.; Chang, L.; Palacios, A. Experimental study on trajectory flame length and axial temperature distribution of inclined turbulent jet flames. *Fire Saf. J.* **2022**, *131*, 103623. [[CrossRef](#)]
12. Xing, C.L.; Huang, X.J.; Wang, J.K.; Zhu, H.; Cheng, C.; Chow, W. Heat transfer from the wall-attached flame to the sidewall composed of different materials. *Int. J. Therm. Sci.* **2023**, *184*, 107918. [[CrossRef](#)]
13. Wang, Q.; Tang, F.; Zhou, Z.; Liu, H.; Palacios, A. Flame height of axisymmetric gaseous fuel jets restricted by parallel sidewalls: Experiments and theoretical analysis. *Appl. Energy* **2017**, *208*, 1519–1526. [[CrossRef](#)]
14. Tao, C.F.; Shen, Y.; Zong, R.W. Experimental study on virtual origins of buoyancy-controlled jet flames with sidewalls. *Appl. Therm. Eng.* **2016**, *106*, 1088–1093. [[CrossRef](#)]
15. Gong, L.; Mo, T.Y.; Han, Y.F.; Zheng, X.W.; Yang, S.N.; Yao, Y.Z.; Zhang, Y.C. Experimental investigation on the behaviors and temperature distribution of cryogenic hydrogen jet flames. *Int. J. Hydrogen Energy* **2023**, *50*, 1062–1074. [[CrossRef](#)]
16. Zhao, C.X.; Li, X.; Wang, X.H.; Li, M.; Xiao, H.H. An experimental study of the characteristics of blended hydrogen-methane non-premixed jet flames. *Process Saf. Environ. Prot.* **2023**, *174*, 838–847. [[CrossRef](#)]
17. Kong, Y.Y.; Li, Y.X.; Wang, S.L.; Han, H.; Duan, P.F.; Yu, X.R.; Han, J.K. Experimental study on jet fire characteristics of hydrogen-blended natural gas. *Int. J. Hydrogen Energy* **2024**, *49*, 1250–1260. [[CrossRef](#)]
18. Li, Y.T.; Kuang, Z.L.; Fan, Z.Y.; Shuai, J. Evaluation of the safe separation distances of hydrogen-blended natural gas pipelines in a jet fire scenario. *Int. J. Hydrogen Energy* **2023**, *48*, 18804–18815. [[CrossRef](#)]
19. He, Q.; Gu, M.Y.; Król, A.; Król, M.; Huang, X.Y.; Tang, F. Pipeline leak jet flame thermal characteristic induced by hydrogen-blended natural gas: Physical modeling of temperature profile based on virtual origin theory. *Int. J. Therm. Sci.* **2023**, *188*, 108220. [[CrossRef](#)]
20. Tang, Z.H.; Wang, Z.R.; Zhao, K. Flame stabilization characteristics of turbulent hydrogen jet flame diluted by nitrogen. *Energy* **2023**, *283*, 129100. [[CrossRef](#)]
21. Lemaire, R.; Menanteau, S. Assessment of radiation correction methods for bare bead thermocouples in a combustion environment. *Int. J. Therm. Sci.* **2017**, *122*, 186–200. [[CrossRef](#)]
22. Zhang, S.J.; Liu, N.; Lei, J.; Xie, X.D.; Jiao, Y.; Tu, R. Experimental study on flame characteristics of propane fire array. *Int. J. Therm. Sci.* **2018**, *129*, 171–180. [[CrossRef](#)]
23. Ji, J.; Li, B.; Wan, H.X.; Ding, L.; Gao, Z.H. Gas temperature rise and flame length induced by two buoyancy-controlled propane burners aligned parallel to the cross wind. *Int. J. Therm. Sci.* **2020**, *152*, 106295. [[CrossRef](#)]
24. Luo, M.C. Effects of radiation on temperature measurement in a fire environment. *J. Fire Sci.* **1997**, *15*, 443–461.
25. Char, J.M.; Yeh, J.H. The measurement of open propane flame temperature using infrared technique. *J. Quant. Spectrosc. Radiat. Transf.* **1996**, *56*, 133–144.
26. Yuen, W.W.; Tien, C.L. A simple calculation scheme for the luminous-flame emissivity. *Proc. Combust. Inst.* **1977**, *16*, 1481–1487. [[CrossRef](#)]
27. Cox, G.; Chitty, R. Some source-dependent effects of unbounded fires. *Combust. Flame* **1985**, *60*, 219–232. [[CrossRef](#)]
28. Tao, C.F.; Liu, B.; Dou, Y.L.; Qian, Y.J.; Zhang, Y.; Meng, S. The experimental study of flame height and lift-off height of propane diffusion flames diluted by carbon dioxide. *Fuel* **2021**, *290*, 119958. [[CrossRef](#)]
29. Tao, C.F.; Shen, Y.; Zong, R.W.; Tang, F. An experimental study of flame height and air entrainment of buoyancy-controlled jet flames with sidewalls. *Fuel* **2016**, *183*, 164–169. [[CrossRef](#)]
30. Dou, Y.L.; Liu, H.Q.; Liu, B.; Zhang, Y.; Liu, Y.Q.; Cheng, X.Z.; Tao, C.F. Effects of carbon dioxide addition to fuel on flame radiation fraction in propane diffusion flames. *Energy* **2021**, *218*, 119552. [[CrossRef](#)]

31. Peng, Q.; Wei, J.; Yang, W.; Jiaqiang, E. Study on combustion characteristic of premixed H<sub>2</sub>/C<sub>3</sub>H<sub>8</sub>/air and working performance in the micro combustor with block. *Fuel* **2022**, *318*, 123676. [[CrossRef](#)]
32. Quintiere, J.G. *Fundamentals of Fire Phenomena*; John Wiley and Sons: Hoboken, NJ, USA, 2006.
33. Gao, Y.K.; Lu, Z.K.; Hua, Y.; Liu, Y.Q.; Tao, C.F.; Gao, W. Experimental study on the flame radiation fraction of hydrogen and propane gas mixture. *Fuel* **2022**, *329*, 125443. [[CrossRef](#)]
34. Sarli, V.D.; Benedetto, A.D. Laminar burning velocity of hydrogen–methane/air premixed flames. *Int. J. Hydrogen Energy* **2007**, *32*, 637–646. [[CrossRef](#)]
35. Hu, E.J.; Huang, Z.H.; He, J.J.; Jin, C.; Zheng, J.J. Experimental and numerical study on laminar burning characteristics of premixed methane–hydrogen–air flames. *Int. J. Hydrogen Energy* **2009**, *34*, 4876–4888. [[CrossRef](#)]
36. Wan, H.X.; Gao, Z.H.; Ji, J.; Fang, J.; Zhang, Y.M. Experimental study on horizontal gas temperature distribution of two propane diffusion flames impinging on an unconfined ceiling. *Int. J. Therm. Sci.* **2019**, *136*, 1–8. [[CrossRef](#)]
37. Lu, Z.K.; Gao, Y.K.; Li, G.C.; Liu, B.; Xu, Y.; Tao, C.F.; Meng, S.; Qian, Y.J. The analysis of temperature and air entrainment rate for the turbulence diffusion jet flame of propane and carbon dioxide gas mixture. *Energy* **2022**, *254*, 124232. [[CrossRef](#)]

**Disclaimer/Publisher’s Note:** The statements, opinions and data contained in all publications are solely those of the individual author(s) and contributor(s) and not of MDPI and/or the editor(s). MDPI and/or the editor(s) disclaim responsibility for any injury to people or property resulting from any ideas, methods, instructions or products referred to in the content.